Short range correlations and the isospin dependence of nuclear correlation functions

R. Cruz-Torres [a], A. Schmidt [a], G.A. Miller [e,∗], L.B. Weinstein [b], N. Barnea [d], R. Weiss [d],
E. Piasetzky [c], O. Hen [a]

[a] *Massachusetts Institute of Technology, Laboratory for Nuclear Science, Cambridge, MA 02139, USA*
[b] *Old Dominion University, Department of Physics, Norfolk, VA 23529, USA*
[c] *Tel Aviv University, School of Physics and Astronomy, Tel Aviv 69978, Israel*
[d] *Hebrew University, Racah Institute of Physics, Jerusalem 91904, Israel*
[e] *University of Washington, Department of Physics, Seattle, WA 98195, USA*

ABSTRACT

Pair densities and associated correlation functions provide a critical tool for introducing many-body correlations into a wide-range of effective theories. *Ab initio* calculations show that two-nucleon pair-densities exhibit strong spin and isospin dependence. However, such calculations are not available for all nuclei of current interest. We therefore provide a simple model, which involves combining the short and long separation distance behavior using a single blending function, to accurately describe the two-nucleon correlations inherent in existing *ab initio* calculations. We show that the salient features of the correlation function arise from the features of the two-body short-range nuclear interaction, and that the suppression of the *pp* and *nn* pair-densities caused by the Pauli principle is important. Our procedure for obtaining pair-density functions and correlation functions can be applied to heavy nuclei which lack *ab initio* calculations.

1. Introduction

Correlation functions are a valuable tool for describing interacting many-body systems, providing a means of encapsulating complex many-body dynamics. In the absence of correlations, a many-body probability density, such as that from a many-body quantum mechanical wave-function, can be written as an anti-symmetrized product of single-particle probability densities. The correlation function describes important deviations from this picture. Our aim here is to explain the basic physics inputs that determine the nuclear pair-density functions and the correlation functions derived from them. This is done by blending the short-distance behavior, as determined by the contact formalism [1–3], with the known long distance behavior. The input needed to use the contact formalism is accessible from experimental data, as shown in Ref. [2].

Correlation functions are widely used in nuclear physics. For recent reviews see Refs. [4,5]. The nucleus is a strongly-interacting, quantum mechanical, many-body system with high density and a complicated interaction between constituent nucleons. There is no fundamental central potential, so correlations must exist. An early paper that modeled nuclear correlation functions [6] was used in a wide variety calculations (see the early review [7]) involving the strong and weak interactions, demonstrating the impact of correlation functions on the field. More recent examples in which correlation functions are crucial ingredients include: calculations of neutrinoless double beta decay [8–13], nuclear transparency in quasielastic scattering [14–19], shadowing in deep inelastic scattering [20], and parity violation in nuclei [21,22].

Despite the wide use of correlation functions, their spin and isospin dependence has received less attention. The nucleon–nucleon interaction is both spin and isospin dependent, and these dependencies become very important at short-range, leading to phenomena such as the strong preference for proton–neutron short-range correlated pairs [23–29].

The calculations in this paper use the formalism of nuclear contacts [2,3] to determine the spin and isospin decomposition of the two-body density that determines the correlation function. This formalism is based on the separation of scales inherent in the long- and short-range structure of nuclei [2,3]. At short distances, the aggregate effect of long-range interactions can be encapsu-
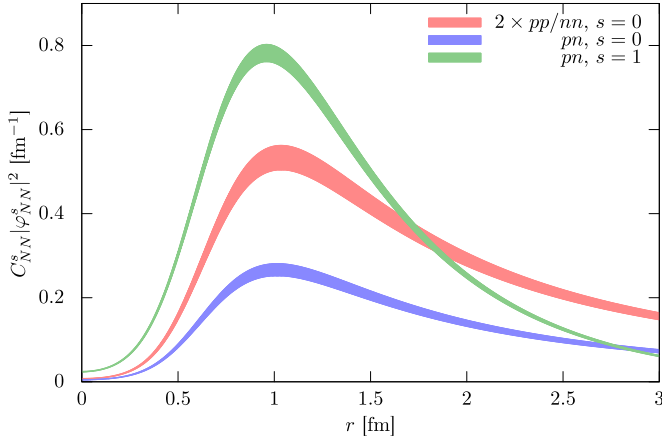
Fig. 1. In the two-body density from contact formalism [2,3], the np two-body density is dominated by spin-1 pairs. ^{40}Ca, shown here, illustrates this universal behavior. For $r \leq 0.9$ fm, these results reproduce those of Cluster Variational Monte Carlo (CVMC) [34] calculations. The pp/nn spin-0 density (peak value 0.5) is enhanced by a factor of 2 to provide some separation from np spin-0. The pn density peaks at 0.2 for spin 0, and 0.8 for spin 1 . (For interpretation of the colors in the figure(s), the reader is referred to the web version of this article.)

lated into coefficients, called "contacts," which are nucleus-specific, while the underlying short-range behavior is a universal property of the two-body nuclear interaction. In the contact formalism, the two-body density, $\rho_{NN,s}(r)$, defining the probability for finding a nucleon–nucleon pair with separation distance r, can be modeled at short distance ($r \lesssim 1$ fm) by:

$$\rho_{NN,s}^{\text{contact}}(r) = C_A^{NN,s} \times |\varphi_{NN,s}(r)|^2 \qquad (1)$$

for nucleus, A, where C_A is the contact coefficient, NN stands for proton–proton (pp), proton–neutron (pn), or neutron–neutron (nn) pairs and the index s denotes the spin $0, 1$ of the two-nucleon systems. The wave functions $\varphi_{NN,s}(r)$ are zero-energy (S- or S-D wave) solutions to the Schrödinger equation with a modern nucleon–nucleon potential, e.g., AV18 [30]. Equation (1) assumes angle averaging, and the zero-energy nature restricts the number of contacts. The key assumption in this formalism is that these functions, $\varphi_{NN,s}(r)$ can be used for all nuclei. Contact coefficients can be determined for the different possible spin and isospin configurations of a nucleon–nucleon pair from experiment or from fitting *ab initio* calculations. Previous studies [2], show that the NN state with deuteron quantum numbers is dominant: the peak value of the product $C_A^{np,s=1}|\varphi_{np,s=1}(r)|^2$ is four times larger than for any other combination. This dominance is caused by the tensor force [31–33] As an example, the decomposition of the two-body density from contact formalism for ^{40}Ca is shown in Fig. 1.

2. Describing the pair (two-body) density

The two-body pair density distribution $\rho_{NN,s}(\vec{r})$, is defined as the probability density for finding a nucleon–nucleon pair separated by $\vec{r}$, with relative spin s, normalized so that its integral is the number of possible NN, s pairs. The two-body density is expressed as a matrix element of the nuclear wave function $|\psi\rangle$ by

$$\rho_{NN,s}(\vec{r}) \equiv \sum_{\substack{i,j \in NN \\ i<j}} \langle \psi | \delta(\vec{r} - \vec{r}_{ij}) P_s | \psi \rangle, \qquad (2)$$

where $\vec{r}_{ij}$ is the separation between nucleons i and j and P_s is a projection operator onto the spin s of the nucleon pair.

Our aim here is to provide a simple understanding of the underlying mechanisms that produce the isospin dependence and

other features. We will compare our results for $\rho_{NN}(r)$ to *ab initio* calculations performed using Cluster Variational Monte Carlo (CVMC) [34] of ^{16}O and ^{40}Ca, the two heaviest nuclei studied so far using CVMC [35]. Several other calculations that include the necessary spin and isospin dependence in computing densities are those of Refs. [31,34,36–39]. A nice *ab initio* treatment of light nuclei has recently appeared [40]. See also Ref. [41], which is based on nuclear matter calculations.

To achieve the desired understanding we design a model in which the two-body density is formed from a combination of the correlated density coming from nuclear contact formalism (Fig. 1), which accounts for the behavior for $r \leq 0.9$ fm and a longer-ranged term, $\rho_{NN}^{(0)}(r)$, for which correlations are expected to be unimportant. We define this term as $\rho_{NN}^{(0)}(r)$, given by

$$\rho_{NN}^{(0)}(\vec{r}) \equiv S_{NN} \int d^3\vec{R}\, \rho_N(\vec{R} + \vec{r}/2)\rho_N(\vec{R} - \vec{r}/2), \qquad (3)$$

where ρ_N is the one-body density, normalized to proton or neutron number, $\vec{R}$ represents the center-of-mass position of a nucleon–nucleon pair, and S_{NN} represents a symmetry factor, which equals 1 for pn pairs, equals $Z(Z-1)/2Z^2$ for pp pairs – since there are only $Z(Z-1)/2$ unique pp pairs in a nucleus – and equals $N(N-1)/2N^2$ for nn pairs.

Then the full two-body density combines the short and long distance behavior, with the relative weighting determined by a blending function, $g_{NN}(r)$, and constant, κ, such that

$$\rho_{NN}(r) = g_{NN}(r)\rho_{NN}^{\text{contact}}(r) + \kappa(1 - g_{NN}(r))\rho_{NN}^{(0)}(r). \qquad (4)$$

We can understand how the correlated and uncorrelated densities contribute to produce the specific behavior of the correlation function seen through CVMC by assessing the quality of this model and by determining the blending function.

In order to parameterize $g_{NN}(r)$, we consider the short- and long-range constraints. At short-distance, where $\rho_{NN}^{\text{contact}}(r)$ is an accurate description of the two-body density [2], $g_{NN}(r)$ equals 1. For large distances, ρ_{NN} must approach $\rho_{NN}^{\text{uncorr.}}$. Since $\rho_{NN}^{\text{contact}}$ falls off approximately as $1/r^2$ for $r > 2$ fm, g_{NN} must approach $(\kappa-1)/\kappa$ in the long-range limit, in order that the pair density approach $\rho_{NN}^{(0)}$. We propose the following model which meets these requirements:

$$g_{NN}(r) = \begin{cases} 1 & r \leq 0.9\text{ fm}, \\ \frac{1}{\kappa}\left(\kappa - 1 + e^{(0.9\text{ fm}-r)/a}\right) & r > 0.9\text{ fm}. \end{cases} \qquad (5)$$

For $r < 0.9$ fm, $\rho_{NN}(r)$ is modeled well by the contact expression Eq. (1) (see [2]). For $r > 0.9$ fm, the contact density and the uncorrelated densities are blended, with a characteristic lengthscale, a. In principle, a would depend on the isospin of the pairs and on the specific nucleus being studied.

Varying the parameters of Eq. (5) to describe pp, nn and pn pairs in ^{16}O and ^{40}Ca shows that the same blending function $g(r)$ can be used to describe all the two-body densities calculated using CVMC, shown in Fig. 2. CVMC correlation functions are shown as points, while our model, described in equation (4), is shown with bands, for which the dominant contribution to the uncertainty comes from the contact coefficients, C_{NN}. The uncorrelated density, $\rho_{NN}^{(0)}$, used by our model is supplied by CVMC calculations of the one-body density ρ_N. The residuals show the difference between the CVMC density and those of the model, divided by the model, with the error bars showing the uncertainties in the CVMC densities. Our model is able to reproduce the correlation functions for both pp and pn pairs in two different nuclei (as these CVMC calculations treat p and n symmetrically, and since ^{16}O and ^{40}Ca
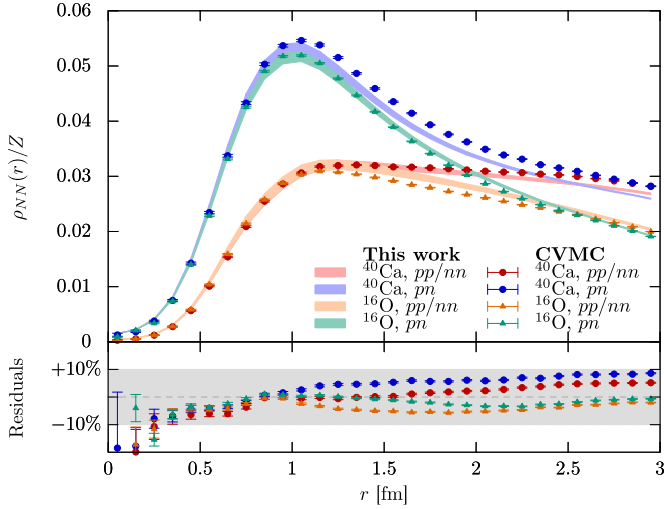
Fig. 2. (Color online) The model of equation (4), with only a single fitted parameter, can reproduce the two-body densities for both *pp* and *pn* pairs, and for both ^{16}O and ^{40}Ca, to within ±10%. The results here are shown for $\kappa = 2$.

are both symmetric nuclei, the results for *pp* and *nn* pairs are the same). In achieving this description we find that the parameter *a* depends smoothly on κ. With $\kappa = 2$, $a = 1.518 \pm 0.001$ fm. Fig. 2 shows that the simple model qualitatively reproduces CVMC calculations.

Fig. 2 demonstrates that the spin-isospin dependence of the two-body density function occur at short distances, and therefore originate from the contact densities of Eq. (1), while the long range behavior is universal between different kinds of pairs and in different nuclei.

3. Correlation function

The standard procedure for defining a correlation function, $F_{NN,s}(r)$, a function of the separation distance between nucleons $r \equiv |\vec{r}|$, is to take the ratio of the fully correlated to the two-body densities computed in the absence of dynamical correlations, i.e.,

$$F_{NN,s}(r) \equiv \frac{\rho_{NN,s}(r)}{\rho_{NN}^{\text{uncorr.}}(r)}. \tag{6}$$

The notation, $F_{NN,s}(r)$, is meant to convey that there can be differences in correlations between different spin and isospin configurations. In cases where we refer to a generic correlation function, we will suppress the indices and use $F(r)$. The denominator must be treated with more sophistication than the function $\rho_{NN}^{(0)}$ used in the phenomenological fit presented above. The correlative effects of the Pauli principle must be included.

Typical applications of correlation functions in nuclear physics begin with anti-symmetrized wave functions, in the form of a Slater determinant. Using a Slater determinant, one can compute the uncorrelated two-body density as the matrix element of the two-body density operator. The result is

$$\rho_{NN}^{\text{uncorr.}}(\vec{r}) = \frac{1}{2} \sum_{\alpha,\beta,\in \text{occ}} \int d^3r_1 d^3r_2 \delta(\vec{r} - (\vec{r}_1 - \vec{r}_2)) \phi_\alpha^\dagger(x_1)\phi_\beta^\dagger(x_2)$$
$$\times [\phi_\alpha(x_1)\phi_\beta(x_2) - \phi_\beta(x_1)\phi_\alpha(x_2)], \tag{7}$$

where x_i represents several quantum numbers: $x \equiv (\vec{r}, m_s = \pm 1/2, m_t = \pm 1/2)$. For the case of proton–neutron pairs, this reduces to the expression of Eq. (3). However, for the case of two protons, one finds:
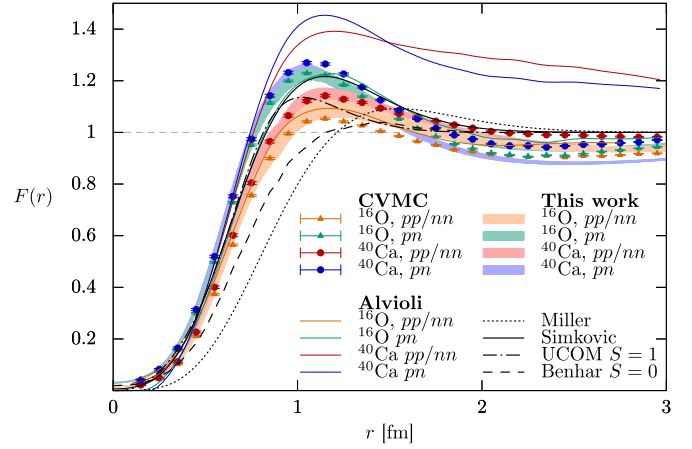
Fig. 3. (Color online) The model of equation (4), with only a single fitted parameter, can reproduce the correlation functions for both *pp* and *pn* pairs, and for both ^{16}O and ^{40}Ca, to within ±10%. The results here are shown for $\kappa = 2$. The predictions of Miller and Spencer [6], Simkovic et al. [12], Alvioli et al. [36], Benhar et al. [41], and the UCOM calculation by Roth et al. [44] are shown for comparison.

$$\rho_{pp}^{\text{uncorr.}}(\vec{r}) = \frac{1}{2} \int d^3r_1 d^3r_2 \delta(\vec{r} - (\vec{r}_1 - \vec{r}_2))$$
$$\times \left[\rho(\vec{r}_1)\rho(\vec{r}_2) - \frac{1}{2}\rho(\vec{r}_1,\vec{r}_2)\rho(\vec{r}_2,\vec{r}_1) \right], \tag{8}$$
$$\equiv \frac{Z}{Z-1}\rho_{pp}^{(0)}(\vec{r}) - \rho_{pp}^{\text{exch.}}(\vec{r}), \tag{9}$$

where $\rho(\vec{r})$ is the proton one-body density, normalized to Z. The expression is the same for neutron–neutron pairs, substituting N for Z and the neutron one-body density for the proton one-body density. The quantity $\rho(\vec{r}_1, \vec{r}_2)$ is the density-matrix defined such that its diagonal elements yield the proton or neutron one-body density. The second term of Eq. (9) represents the influence of the Pauli exclusion principle: two spin-up protons cannot occupy the same orbital. This term is absent for the neutron–proton two-body density.

It is useful to avoid using a specific Slater determinant, which would depend on the nucleus. Instead, we apply a result based on nuclear matter (but using a local-density approximation) expressed as

$$\rho_{NN}^{\text{exch.}}(\vec{r}) = \frac{Z}{2(Z-1)}\rho_{pp}^{(0)}(r) \times \left(\frac{3j_1(\bar{k}_F r)}{\bar{k}_F r} \right)^2, \tag{10}$$

where $\bar{k}_F$ is a Fermi momentum (averaged over the nuclear volume) and j_1 is a spherical Bessel function. We use this approximation throughout, with $\bar{k}_F$ assumed to be 200 MeV/c. This approximation amounts to using the local-density approximation to the first term of the density-matrix expansion of Ref. [42]. We verify the accuracy of Eq. (10) numerically, by comparing with the Slater determinant provided by the single-particle wave functions of Ref. [43].

The points in Fig. 3 show correlation functions calculated using equations (3), (10), and (6), with CVMC providing the one- and two-body densities. As can be seen, the correlation functions are similar for ^{16}O and ^{40}C. But there is some isospin dependence, as displayed by the differences at $r < 1.5$ fm between *pp*- and *pn*-pairs (dominated by $s = 1$). Note also that because these CVMC calculations treat *p* and *n* symmetrically, and since $N = Z$ for both ^{16}O and ^{40}Ca, the results for *pp* and *nn* pairs are the same.

Fig. 3 also shows, for comparison, several other calculations of nuclear correlation functions, including the original model sug-

Table 1
Parameters describing $F(r)$, using the functional form of equation (11).

Parameter	Units	Value (pp/nn)	Value (pn)
α	fm^{-2}	3.17	1.08
γ	–	0.995	0.985
β_1	fm^{-2}	1.81	−0.432
β_2	fm^{-3}	5.90	−3.30
β_3	fm^{-4}	−9.87	2.01
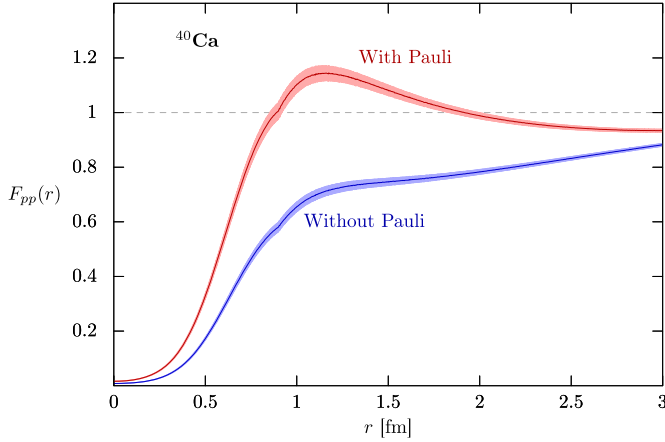
Fig. 4. Pauli exchange has a significant effect on pp and nn correlations. Correlations taken relative to a classical uncorrelated density (blue) (Eq. (3)) appear significantly suppressed compared to correlations taken relative to an uncorrelated density that includes Pauli exchange (red).

gested by Miller and Spencer [6] as well as more recent work. The correlation functions from *ab initio* and from our model are close to that of Simkovic et al. [12] and to the ^{16}O calculations of Alvioli et al. [36], but are higher than the correlation functions predicted by Benhar et al. [41] and by Miller and Spencer. The calculations by Alvioli et al. for ^{40}Ca predict a significantly higher correlation function for both pp/nn and pn. A calculation using the Unitary Correlation Operator Method (UCOM) [44] in the $T = 0$, $S = 1$ channel is slightly lower than our predictions for pn pairs. A study of Jastrow correlation functions [45] is relevant in the present context. These comparisons show that at the level of two-body cluster truncation, isospin symmetry is broken, and that the Miller–Spencer parameterization suffers from this problem. The Simkovic et al. model avoids this problem because of the bump (at about $r = 1$ fm) in their correlation function. Our present reproduction of the correlation function of [12] shows that our work also avoids this problem. It is necessary to keep the effects of the Pauli principle in mind when making comparisons between correlation functions produced by different authors.

For convenience, we provide the following parameterization for the pp/nn and pn correlation functions determined from CVMC:

$$F(r) = 1 - e^{-\alpha r^2} \times \left(\gamma + r \sum_{i=1}^{3} \beta_i r^i \right) \qquad (11)$$

with parameter values given in Table 1. This function reproduces the correlation functions of both ^{16}O and ^{40}Ca.

Note that the Figs. 1 and 3 display a striking contrast. The huge differences between like and un-like nucleon pairs seen in the former figure do not show up in the latter figure. This is because of the influence of the Pauli principle (as manifest in the second term of Eq. (9)), which strongly enhances the pp and nn correlation functions defined in Eq. (6). This effect is displayed in Fig. 4.

4. Discussion

Our model, defined in Eq. (4) and Eq. (5), for the pair-density (Eq. (2)) requires the minimal input of the blending function, the nuclear contact coefficients and the universal functions $|\varphi_{NN,s}(r)|^2$ of Eq. (1). The isospin-dependence of the two-body pair density is produced by short-ranged interactions, driven by the two-nucleon tensor force. While the nuclear contacts used in this work were determined from CVMC calculations, they can also be determined from experimental data, as shown in Ref. [2]. Thus one may obtain the pair-density for heavy nuclei for which *ab initio* calculations do not exist.

The correlation function, Eq. (6), can also be obtained. One needs a one-body density function to form $\rho_{NN}^{(0)}(r)$. The effects of the Pauli principle must be included as (for example) in Eq. (10). One-body densities have been well-measured experimentally, and simple parameterizations exist for many different nuclei, e.g., Ref. [46].

In summary, we have provided a procedure that enables predictions of two-body densities and correlation functions for nuclei that are too large for adequate *ab initio* calculations.

Acknowledgements

References

[1] S. Tan, Ann. Phys. 323 (2008) 2952–2987.
[2] R. Weiss, R. Cruz-Torres, N. Barnea, E. Piasetzky, O. Hen, The nuclear contacts and short range correlations in nuclei, Phys. Lett. B 780 (2018) 211–215.
[3] R. Weiss, B. Bazak, N. Barnea, Generalized nuclear contacts and momentum distributions, Phys. Rev. C 92 (2015) 054311.
[4] O. Hen, G.A. Miller, E. Piasetzky, L.B. Weinstein, Nucleon–nucleon correlations, short-lived excitations, and the quarks within, Rev. Mod. Phys. 89 (2017) 045002.
[5] C. Ciofi degli Atti, In-medium short-range dynamics of nucleons: recent theoretical and experimental advances, Phys. Rep. 590 (2015) 1–85.
[6] G.A. Miller, J.E. Spencer, A survey of pion charge-exchange reactions with nuclei, Ann. Phys. 100 (1976) 562.
[7] W.C. Haxton, G.J. Stephenson, Double beta decay, Prog. Part. Nucl. Phys. 12 (1984) 409–479.
[8] M. Kortelainen, O. Civitarese, J. Suhonen, J. Toivanen, Short-range correlations and neutrinoless double beta decay, Phys. Lett. B 647 (2007) 128–132.
[9] M. Kortelainen, J. Suhonen, Improved short-range correlations and $0\nu\beta\beta$ nuclear matrix elements of ^{76}Ge and ^{82}Se, Phys. Rev. C 75 (2007) 051303.
[10] M. Kortelainen, J. Suhonen, Nuclear matrix elements of $0\nu\beta\beta$ decay with improved short-range correlations, Phys. Rev. C 76 (2007) 024315.
[11] J. Menendez, A. Poves, E. Caurier, F. Nowacki, Disassembling the nuclear matrix elements of the neutrinoless beta beta decay, Nucl. Phys. A 818 (2009) 139–151.
[12] F. Šimkovic, A. Faessler, H. Müther, V. Rodin, M. Stauf, $0\nu\beta\beta$-decay nuclear matrix elements with self-consistent short-range correlations, Phys. Rev. C 79 (2009) 055501.
[13] J. Engel, G. Hagen, Corrections to the neutrinoless double-β-decay operator in the shell model, Phys. Rev. C 79 (2009) 064317.
[14] I. Mardor, Y. Mardor, E. Piasetzky, J. Alster, M.M. Sargsian, Effect of multiple scattering on the measurement of nuclear transparency, Phys. Rev. C 46 (1992) 761–767.
[15] S. Frankel, W. Frati, N. Walet, Extracting nuclear transparency from p-A cross-sections, Nucl. Phys. A 580 (1994) 595–613.
[16] B. Kundu, P. Jain, J.P. Ralston, J. Samuelsson, Hadronic electromagnetic form-factors and color transparency, in: Perspectives in Hadronic Physics. Proceedings, 2nd International Conference, Trieste, Italy, May 10–14, 1999, pp. 87–96.

[17] B. Kundu, J. Samuelsson, P. Jain, J.P. Ralston, Perturbative color transparency in electroproduction experiments, Phys. Rev. D 62 (2000) 113009.

[18] T.S.H. Lee, G.A. Miller, Color transparency and high-energy (p, 2 p) nuclear reactions, Phys. Rev. C 45 (1992) 1863–1870.

[19] W. Cosyn, M.C. Martínez, J. Ryckebusch, Color transparency and short-range correlations in exclusive pion photo- and electroproduction from nuclei, Phys. Rev. C 77 (2008) 034602.

[20] G. Baym, B. Blättel, L.L. Frankfurt, H. Heiselberg, M. Strikman, Correlations and fluctuations in high-energy nuclear collisions, Phys. Rev. C 52 (1995) 1604–1617.

[21] E.G. Adelberger, W.C. Haxton, Parity violation in the nucleon–nucleon interaction, Annu. Rev. Nucl. Part. Sci. 35 (1985) 501–558.

[22] I.S. Towner, Quenching of spin matrix elements in nuclei, Phys. Rep. 155 (1987) 263–377.

[23] A. Tang, J.W. Watson, J. Aclander, et al., n-p short range correlations from (p, 2p + n) measurements, Phys. Rev. Lett. 90 (2003) 042301.

[24] E. Piasetzky, M. Sargsian, L. Frankfurt, M. Strikman, J.W. Watson, Evidence for strong dominance of proton–neutron correlations in nuclei, Phys. Rev. Lett. 97 (2006) 162504.

[25] R. Shneor, P. Monaghan, R. Subedi, et al., Investigation of proton–proton short-range correlations via the ^{12}C$(e, e'pp)$ reaction, Phys. Rev. Lett. 99 (2007) 072501.

[26] R. Subedi, R. Shneor, P. Monaghan, et al., Probing cold dense nuclear matter, Science 320 (2008) 1476–1478.

[27] I. Korover, N. Muangma, O. Hen, et al., Probing the repulsive core of the nucleon–nucleon interaction via the ^{4}He$(e, e'pn)$ triple-coincidence reaction, Phys. Rev. Lett. 113 (2014) 022501.

[28] O. Hen, M. Sargsian, L.B. Weinstein, et al., Momentum sharing in imbalanced Fermi systems, Science 346 (2014) 614–617.

[29] M.M. Sargsian, New properties of the high-momentum distribution of nucleons in asymmetric nuclei, Phys. Rev. C 89 (2014) 034305.

[30] R.B. Wiringa, V.G.J. Stoks, R. Schiavilla, An accurate nucleon–nucleon potential with charge independence breaking, Phys. Rev. C 51 (1995) 38–51.

[31] M. Alvioli, C. Ciofi degli Atti, H. Morita, Proton-neutron and proton–proton correlations in medium-weight nuclei and the role of the tensor force, Phys. Rev. Lett. 100 (2008) 162503.

[32] R. Schiavilla, R.B. Wiringa, S.C. Pieper, J. Carlson, Tensor forces and the ground-state structure of nuclei, Phys. Rev. Lett. 98 (2007) 132501.

[33] M.M. Sargsian, T.V. Abrahamyan, M.I. Strikman, L.L. Frankfurt, Exclusive electro-disintegration of He-3 at high Q2. II. Decay function formalism, Phys. Rev. C 71 (2005) 044615.

[34] S.C. Pieper, R.B. Wiringa, V.R. Pandharipande, Variational calculation of the ground state of O-16, Phys. Rev. C 46 (1992) 1741–1756.

[35] D. Lonardoni, A. Lovato, S.C. Pieper, R.B. Wiringa, Variational calculation of the ground state of closed-shell nuclei up to $A = 40$, arXiv:1705.04337 [nucl-th], 2017.

[36] M. Alvioli, C. Ciofi degli Atti, H. Morita, Ground-state energies, densities and momentum distributions in closed-shell nuclei calculated within a cluster expansion approach and realistic interactions, Phys. Rev. C 72 (2005) 054310.

[37] M. Alvioli, C. Ciofi degli Atti, H. Morita, Proton–proton and proton–neutron correlations in medium-weight nuclei: role of the tensor force within a many-body cluster expansion, in: Annual HPC-Europa Meeting Bologna, Italy, July 14–17, 2007.

[38] M. Alvioli, M. Strikman, C. Ciofi degli Atti, Realistic nuclear wave functions and heavy ion collisions, in: HPC-Europa2 Montpellier, France, October 14–16, 2009.

[39] H. Feldmeier, W. Horiuchi, T. Neff, Y. Suzuki, Universality of short-range nucleon–nucleon correlations, Phys. Rev. C 84 (2011) 054003.

[40] S. Pastore, J. Carlson, V. Cirigliano, et al., Neutrinoless Double Beta Decay Matrix Elements in Light Nuclei, 2017.

[41] O. Benhar, R. Biondi, E. Speranza, Short-range correlation effects on the nuclear matrix element of neutrinoless double-β decay, Phys. Rev. C 90 (2014) 065504.

[42] J.W. Negele, D. Vautherin, Density-matrix expansion for an effective nuclear Hamiltonian, Phys. Rev. C 5 (1972) 1472–1493.

[43] J.W. Negele, Structure of finite nuclei in the local-density approximation, Phys. Rev. C 1 (1970) 1260–1321.

[44] R. Roth, H. Hergert, P. Papakonstantinou, T. Neff, H. Feldmeier, Matrix elements and few-body calculations within the unitary correlation operator method, Phys. Rev. C 72 (2005) 034002.

[45] J. Engel, J. Carlson, R.B. Wiringa, Jastrow functions in double-β decay, Phys. Rev. C 83 (2011) 034317.

[46] H. De Vries, C.W. De Jager, C. De Vries, Nuclear charge and magnetization density distribution parameters from elastic electron scattering, At. Data Nucl. Data Tables 36 (1987) 495–536.